OPEN ACCESS

Short report

Congenital anaemia associated with loss-of-function variants in DNA polymerase epsilon 1

Ichiro Takeuchi,[1] Kanako Tanase-Nakao,[2] Ayame Ogawa ,[3,4] Tohru Sugawara,[5] Osuke Migita,[6,7] Makoto Kashima,[8] Touko Yamazaki,[9] Akihiro Iguchi,[10] Yasuhiro Naiki,[11] Toru Uchiyama,[12] Junya Tamaoki,[13] Hiroki Maeda,[13] Hirotaka Shimizu,[1] Toshinao Kawai,[14] Kosuke Taniguchi ,[6] Hiromi Hirata,[8] Makoto Kobayashi,[13] Kimikazu Matsumoto,[10] Kiyoshi Naruse,[9] Kenichiro Hata,[6] Hidenori Akutsu,[5] Takashi Kato,[3,4] Satoshi Narumi,[2] Katsuhiro Arai,[1] Akira Ishiguro [10,15]

► Additional supplemental material is published online only. To view, please visit the journal online (http://dx.doi.org/10.1136/jmg-2023-109444).

For numbered affiliations see end of article.

Correspondence to
Dr Akira Ishiguro, National Center for Child Health and Development, Setagaya-ku, Japan; ishiguro-a@ncchd.go.jp

Received 2 June 2023
Accepted 25 September 2023
Published Online First 13 October 2023

To cite: Takeuchi I, Tanase-Nakao K, Ogawa A, *et al*. *J Med Genet* 2024;**61**:239–243.

SUMMARY

DNA polymerase epsilon (Pol ε), a component of the core replisome, is involved in DNA replication. Although genetic defects of Pol ε have been reported to cause immunodeficiency syndromes, its role in haematopoiesis remains unknown. Here, we identified compound heterozygous variants (p.[Asp1131fs];[Thr1891del]) in *POLE*, encoding Pol ε catalytic subunit A (POLE1), in siblings with a syndromic form of severe congenital transfusion-dependent anaemia. In contrast to Diamond-Blackfan anaemia, marked reticulocytopenia or marked erythroid hypoplasia was not found. Their bone marrow aspirates during infancy revealed erythroid dysplasia with strongly positive TP53 in immunostaining. Repetitive examinations demonstrated trilineage myelodysplasia within 2 years from birth. They had short stature and facial dysmorphism. HEK293 cell-based expression experiments and analyses of patient-derived induced pluripotent stem cells (iPSCs) disclosed a reduced mRNA level of Asp1131fs-POLE1 and defective nuclear translocation of Thr1891del-POLE1. Analysis of iPSCs showed compensatory mRNA upregulation of the other replisome components and increase of the TP53 protein, both suggesting dysfunction of the replisome. We created *Pole*-knockout medaka fish and found that heterozygous fishes were viable, but with decreased RBCs. Our observations expand the phenotypic spectrum of the Pol ε defect in humans, additionally providing unique evidence linking Pol ε to haematopoiesis.

INTRODUCTION

DNA replication is an accurate process governed by a multi-protein complex, named a 'replisome', which unwinds double-stranded DNA and duplicates the strands. DNA polymerase epsilon (Pol ε), a member of the core replisome, is composed of four subunits, namely, catalytic subunit A (POLE1) and three other subunits (POLE2 to POLE4) with distinct structural roles. A mouse model of Pol ε hypomorphy (*Pole4*$^{-/-}$) presents systemic manifestations, including leucopenia, anaemia and increased frequency of lymphoma, suggesting the role of Pol ε in haematopoiesis.[1] In humans, genetic variants leading to Pol ε deficiency were first described in a large consanguineous French family with FILS (*f*acial dysmorphism, *i*mmunodeficiency, *l*ivedo and *s*hort stature) syndrome (MIM*615139).[2] The patients had a homozygous variant (c.4444+3A>G) in *POLE* (MIM*174762), encoding the POLE1 protein, that resulted in 90% reduction of the mature protein. No major haematological abnormalities other than immunodeficiency were observed in the French family, whereas pancytopenia and myelodysplasia were observed in the second (Palestinian) family.[3] More recently, combinations of a seemingly non-functional *POLE* variant and deep intronic variant (c.1226+234G>A or c.1686+32C>G) were shown to cause another multisystem disorder named IMAGE-I (*i*ntrauterine growth restriction (IUGR), *m*etaphyseal dysplasia, *a*drenal hypoplasia congenita, *g*enital anomalies and *i*mmunodeficiency) syndrome (MIM*618336).[4] Patients with IMAGE-I syndrome were reported to have immunodeficiency and lymphoma, but no major haematological abnormalities. Collectively, although a relationship between Pol ε and haematopoiesis has been speculated in humans, no clear evidence has yet been established.

Here, we describe Japanese siblings with novel compound heterozygous *POLE* variants (p.[Asp1131fs];[Thr1891del]), both located in the protein-coding exons. Both siblings commonly had congenital anaemia without immunodeficiency.

SUBJECTS AND METHODS

Patient 1 (P1) was a Japanese female patient followed up for IUGR and was born at 29 weeks of gestation with a weight of 726 g (−3.3 SD) and a height of 32 cm (−2.9 SD). At birth, she had severe macrocytic anaemia without reticulocytopenia (red blood cells (RBCs) 0.95×10^{12}/L, haemoglobin (Hgb) level 43 g/L, mean corpuscular volume (MCV) 123 fL, reticulocyte counts 158×10^{9}/L, white blood cells (WBCs) 2.3×10^{9}/L, and platelets 396×10^{9}/L). Patient 2 (P2), the younger sibling of P1, also had IUGR and was born at 37 weeks of gestation with a weight of 2124 g (–1.6 SD) and height of 43 cm (–1.9 SD). Her Hgb level was 54 g/L at birth; there were no decreases in reticulocyte counts, WBC

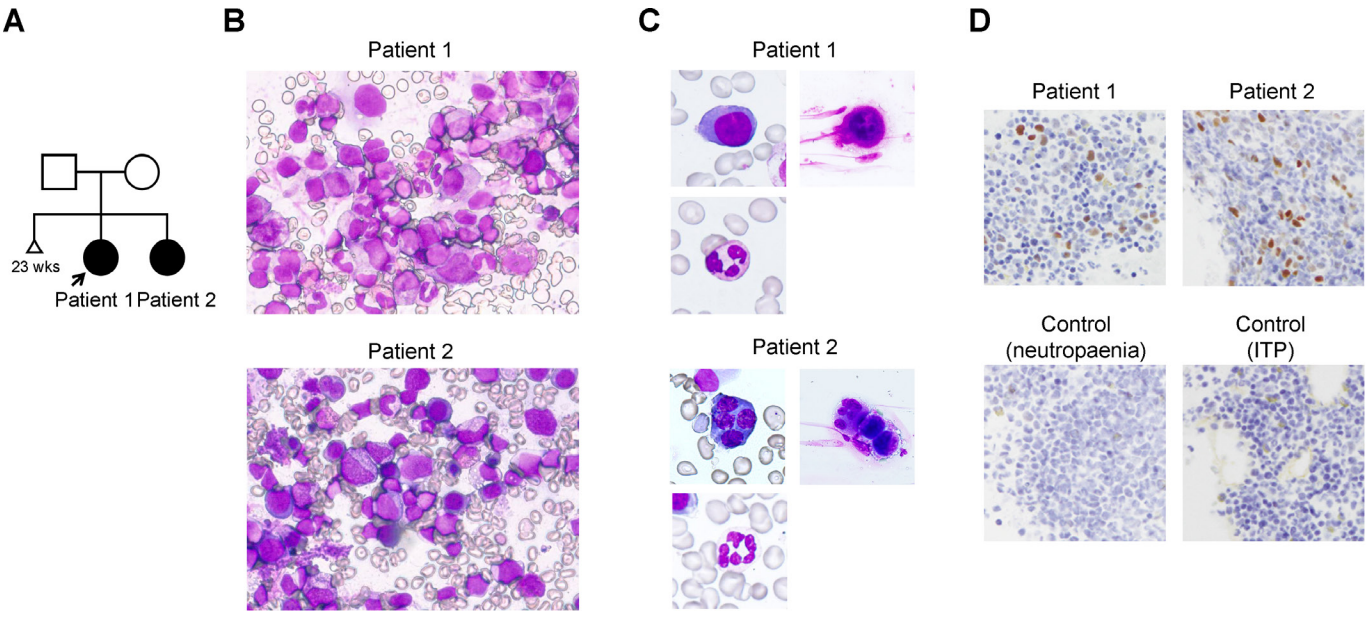

Figure 1 Clinical phenotypes of the patients. (A) The pedigree of patients 1 and 2. (B) Myelograms with May-Giemsa staining of tissues of patient 1 and patient 2 in infancy show erythroid dysplasia without marked erythroid hypoplasia. (C) Myelograms with May-Giemsa staining of tissues of patient 1 and patient 2 in toddlerhood show dysplastic changes, such as hypersegmented neutrophils, megaloblastic change, multinucleated erythroblasts and micromegakaryocytes. (D) Immunostaining for TP53 using clot sections of the bone marrow from patients 1 and 2 demonstrate strongly positive signals compared with those of a patient with immune thrombocytopenia (ITP) in early childhood and a patient with autoimmune neutropaenia in infancy.

counts or platelet counts (RBC 1.71×10^{12}/L, MCV 117 fL, reticulocyte counts 30×10^{9}/L, platelets 306×10^{9}/L and WBC 12.8×10^{9}/L). Their haematological characteristics are shown in online supplemental table 1 and online supplemental figures 1 and 2. Their parents were healthy and non-consanguineous (figure 1A). Despite congenital anaemia, marked reticulocytopenia or erythroid hypoplasia was not found, in contrast to that observed in Diamond-Blackfan anaemia (MIM*105650). They required monthly transfusions of RBCs. Examinations of bone marrow aspirates during infancy showed erythroid dysplasia, but without marked erythroid hypoplasia (figure 1B). Their follow-up examinations demonstrated hyperplastic marrow with trilineage myelodysplasia and excess blasts (P1, 7.5%; P2, 8.0%) that fit myelodysplastic syndrome (MDS), classified into refractory anaemia with excess blasts −1 using the WHO classification within 2 years from birth (figure 1C). No chromosomal abnormalities were found associated with MDS, including monosomy 7 and trisomy 8. Immunostaining for TP53 in their bone marrow cells showed enhanced signals compared with controls (figure 1D). Additional features included short stature and epicanthic folds as facial anomalies; however, they did not have adrenal insufficiency, genitourinary anomalies or café-au-lait patches. The immunological characteristics of the two patients are shown in online supplemental table 2. P1 had decreased $CD8^{+}$ cytotoxic T cells, but no obvious abnormalities in other subsets. Although the data of P2 was evaluated in post-MDS, there was no obvious loss of subsets and the antibody production was maintained. P1 and P2 had no symptoms associated with immunodeficiency. P1 developed bloody diarrhoea, and inflammatory bowel disease (unclassified) was subsequently diagnosed during infancy. P1 also had microencephaly and skull thickening. Clinical features of P1 and P2 compared with those with FILS and IMAGE-I syndromes are summarised in online supplemental table 3. Full descriptions of clinical information are available in online supplemental data.

Exome sequencing of the patients and their parents was performed with SureSelect Human All Exome V6 (Agilent Technologies, Santa Clara, California, USA) and the Illumina HiSeq 2500 system (Illumina, San Diego, California, USA). We filtered the dataset using the Japanese variant database JPN38K (https://jmorp.megabank.tohoku.ac.jp/). To obtain a list of candidate pathogenic variants, the following filtering criteria were applied: (1) non-synonymous or frameshift variants in coding exons or splicing sites, (2) allele frequencies below 0.5% in 38KJPN, and (3) absence of the variant in our in-house exome data to filter pipeline-specific systematic errors. Potential pathogenicity was assumed from inheritance patterns—de novo, homozygous, compound heterozygous or hemizygous—and functional effects were predicted using SIFT, PolyPhen2 and CADD. Direct sequencing was performed to confirm the presence of the identified *POLE* variants.

Structural data of yeast Pol ε and human replisome were retrieved from the Protein Data Bank (https://www.rcsb.org/). Doxycycline-inducible stable HEK293 cells expressing N-terminal haemagglutinin-tagged POLE1 were established with previously described methods.[5] Induced pluripotent stem cells (iPSCs) were established from a small intestinal tissue biopsy specimen from the proband, P1, and peripheral blood mononuclear cells from P2. Clones were established for P1 (three) and P2 (one). Two iPSC lines, each created from healthy individuals, were used as controls. Total RNA samples prepared from iPSCs were subjected to RNA sequencing (RNA-seq). Antibodies against haemagglutinin, human POLE2 and human TP53 were used for western blotting and immunofluorescence imaging. We generated two lines of *Pole*-deficient medaka (*Oryzias latipes*) using CRISPR/Cas9 genome editing. To assess pre-hatching stunting, we observed the embryo at 7 days after fertilisation using hatching enzymes. Peripheral blood was collected from the bulbus arteriosus of fish using glass capillaries, and cells were counted with a haemocytometer.

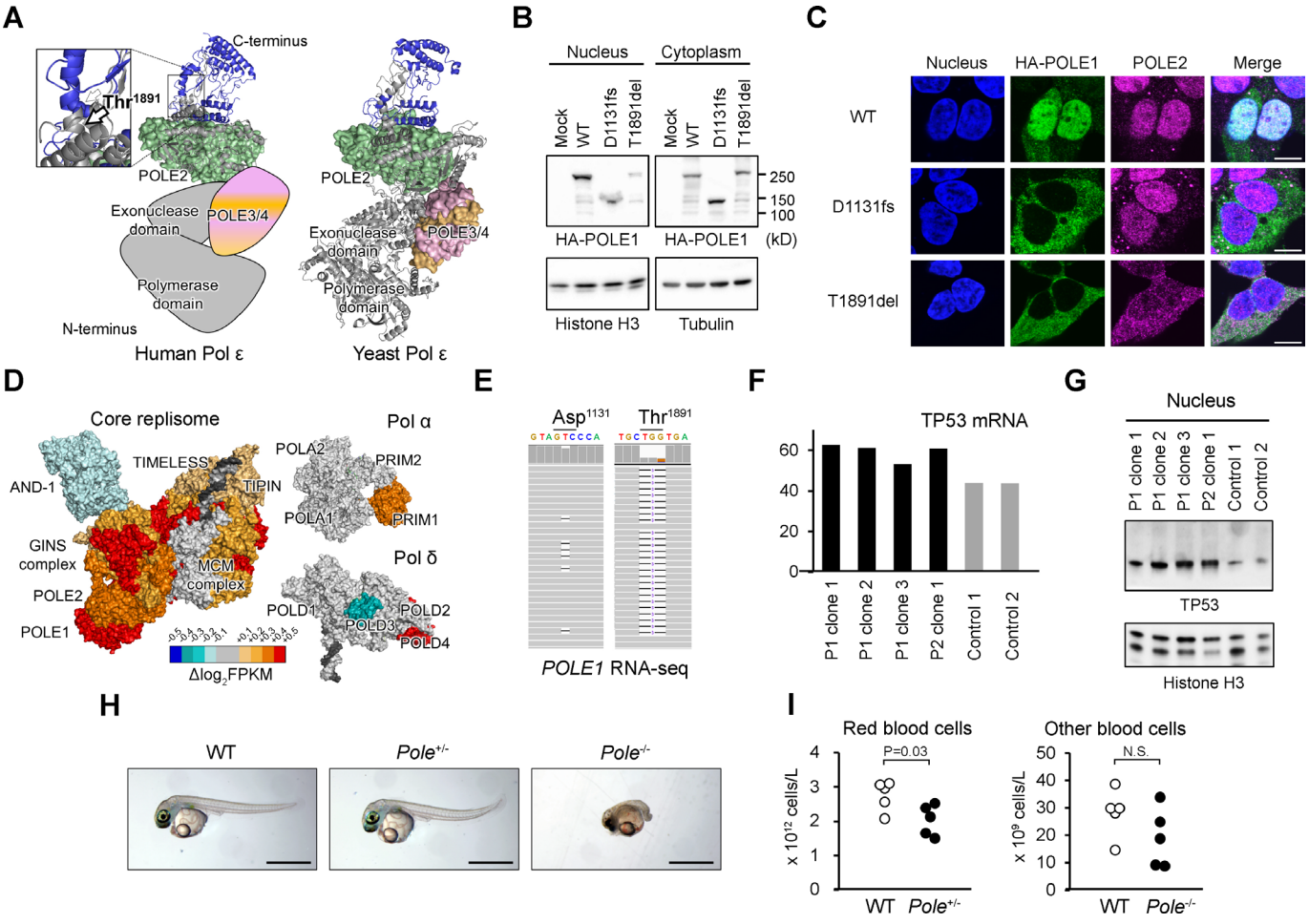

Figure 2 Functional characterisation of the *POLE* variants. (A) Three-dimensional structure of human and yeast Pol ε. Due to incomplete cryo-electron microscopy data for human Pol ε, the overall structure was inferred based on the tetrameric structure of yeast pol ε. POLE1 is shown in grey and the residues whose spatial arrangement would be affected by deletion of Thr1891 (indicated by an arrow) are shown in blue. (B) Western blot of nuclear and cytoplasmic extracts of HEK293 cells expressing haemagglutinin (HA)-tagged POLE1 variants. Histone H3 and tubulin are loading controls of nuclear and cytoplasmic extracts, respectively. (C) Immunofluorescence images, showing the subcellular localisation of HA-POLE1 and endogenous POLE2. Nuclei were stained with Hoechst 33342. Scale bars indicate 10 µm. (D) Relative mRNA expression levels of components of the core replisome, Pol α and Pol δ are indicated. Differences of mean $\log_2$ fragments per kilobase million (FPKM) values between patient's iPSCs and controls are indicated by colours. (E) RNA-seq read data derived from iPSC of P1, showing reads corresponding to the two *POLE* variants (Asp1131fs and Thr1891del). (F) TP53 mRNA expression levels of iPSCs are shown in FPKM. (G) TP53 protein expression levels of iPSCs were assessed with Western blotting. (H) Genome-edited *Pole*-knockout medaka fish. Homozygous fish showed early embryonic lethality. (I) Counts of blood cells of heterozygous *Pole*-knockout medaka and controls. iPSCs, induced pluripotent stem cells; WT, wildtype.

Details of experimental methods are described in online supplemental data and supplemental figures 3-5.

RESULTS

Our exome sequencing revealed that both P1 and P2 carried compound heterozygous *POLE* variants: NM_006231.2:c.3392del, p.Asp1131Alafs*24 and c.5672_5674del, p.Thr1891del (ClinVar accession number: SCV003806449 and SCV003806448, respectively). No other candidate variants were found in any genes implicated in congenital anaemia, including 71 causative genes of Fanconi anaemia, Diamond-Blackfan anaemia, Swachmann-Diamond syndrome, congenital dyserythropoietic anaemia and other syndromes, including *TP53*, *SAMD9*, *GATA1* and *GATA2*. These two variants were not observed in 38 000 healthy Japanese individuals (https://jmorp.megabank.tohoku.ac.jp/). The p.Asp1131fs variant, if translated, would lose 51% of the amino acid sequence and was considered non-functional. The p.Thr1891del variant was predicted to have a single residue deletion located in the centre of an α-helix (figure 2A), likely affecting the spatial arrangement of approximately 400 residues after the helix (figure 2A, coloured in blue).

We tested the pathogenicity of the two variants in vitro. Western blotting of the cytoplasmic and nuclear extracts of HEK293 cells expressing each POLE1 variant showed markedly decreased amounts of the two variants in the nuclear extracts (figure 2B). Immunofluorescence recapitulated the impaired nuclear localisation of the two variants (figure 2C). Intriguingly, endogenous POLE2 protein failed to localise at the nucleus in cells expressing Thr1891del-POLE1 (figure 2C).

We performed transcriptome analysis with patient-derived iPSCs. The mRNA levels of 12 out of the 17 human core replisome components were increased by more than 15% in the patients' cells (figure 2D). This putative compensation was restricted to the core replisome, but was not observed in Pol α or Pol δ. POLE1 mRNA level was increased by approximately 50%,

although the transcript from the p.Asp1131fs allele was depleted (figure 2E). This suggests that mRNA with p.Asp1131fs was degraded via nonsense-mediated decay, and the p.Thr1891del allele was expressed at approximately threefold higher level compared with normal. As the loss of Pol ε could lead to replication stress and DNA damage, we addressed whether TP53 was upregulated in the patients' iPSCs and showed a trend toward higher expression in patients' cells (figure 2F). Western blotting further displayed a clear upregulation of TP53 protein in patients' cells (figure 2G).

Finally, we studied the effect of POLE1 deficiency on haematopoiesis using the medaka (*O. latipes*). Homozygous *Pole*-knockout (KO) fish and some heterozygous fish showed early embryonic lethality (figure 2H). In morphologically normal *Pole*$^{+/-}$ fish, the number of RBCs in the peripheral blood was significantly decreased (p=0.03), whereas a number of other blood cells were comparable to those in the wildtype fish (figure 2I).

DISCUSSION

We identified novel compound heterozygous *POLE* variants (p.[Asp1131fs];[Thr1891del]) in siblings with severe congenital anaemia. This may be the first report to demonstrate that *POLE* mutations could be a potential cause of congenital anaemia, which constitutes the most severe phenotype of Pol ε dysfunction and the consequential TP53 hyperexpression.

The analyses using HEK293 cells and patient-derived iPSCs confirmed the loss of function of the p.Asp1131fs and p.Thr1891del variants: POLE1 mRNA level was decreased in the p.Asp1131fs variant and nuclear translocation was defective in the p.Thr1891del variant. Thr1891del-POLE1 was predicted to retain most of the binding surface to POLE2 and might be able to sequester POLE2 in the cytoplasm. Previous studies found that patients with FILS syndrome and IMAGE-I syndrome were still able to produce reduced amounts of non-mutated POLE1; however, our patients were unable to produce any non-mutated protein.[2 4] Indeed, heterozygous *POLE* variants (p.[Asp1131fs];[Thr1891del]) might result in more severe phenotypes than the replication stress-related phenotypes observed in FILS syndrome and IMAGE-I syndrome. POLE1 is ubiquitously expressed (Human Protein Atlas, proteinatlas.org) and the reported IMAGE-I syndrome had variability in phenotypes.[4] Haematopoietic cells with high DNA synthesis are susceptible to the Pol ε defect, and intrauterine growth retardation and short stature after birth could be attributed to the ubiquitous POLE1 expression. No adrenal insufficiency and only epicanthic folds as facial abnormalities until the present age in our patients could be within the variability of IMAGE-I syndrome.

The pathophysiology of haematological abnormalities in our patients was not confirmed; however, intravascular and extravascular haemolysis was less involved in the congenital anaemia based on the laboratory data (online supplemental table 1). We did not observe burr/helmet cells in the peripheral blood, splenomegaly, increased reticulocyte counts/lactate dehydrogenase/bilirubin/urinary urobilinogen or decreased haptoglobin. Despite the low growth rate of patient-derived iPSCs, we believe the contribution of impaired regenerative anaemia was limited. Marked reticulocytopenia or erythroid hypoplasia was not found, in contrast to that observed in Diamond-Blackfan anaemia. The clinical course in which they had severe anaemia at birth and developed myelodysplasia later indicates that anaemia was not caused by the MDS associated with somatic mutations. The consequent TP53 overexpression leading to the apoptosis suggests an association of ineffective haematopoiesis, as in other disorders related to congenital anaemia or inherited bone marrow failure.[6–10] In Fanconi anaemia, the hyperactivation of TP53 or TP21 before and after birth by replicative or cellular stress is considered the major factor leading to apoptosis and impaired haematopoietic stem cell expansion.[7] In Diamond-Blackfan anaemia and 5q– syndrome, the myelogram of patients also shows TP53 hyperexpression, and animal experiments have revealed the improvement of haematological abnormalities following *p53* KO.[8–10] The associated TP53 activation has been observed in fibroblasts from patients with IMAGE-I, and the phenotypes of size reduction and lymphopenia in KO-POLE4 mice were improved by *p53* KO.[1]

This report was based on siblings in one family and a limited functional analysis due to the low growth rate of patient-derived iPSCs and embryonic lethality of *Pole*-KO fish; nevertheless, our observations not only expand the phenotypic spectrum of the human Pol ε defect but also provide unique evidence linking Pol ε and haematopoiesis.

Author affiliations
[1]Center for Pediatric Inflammatory Bowel Disease, Division of Gastroenterology, National Center for Child Health and Development, Tokyo, Japan
[2]Department of Molecular Endocrinology, National Research Institute for Child Health and Development, Tokyo, Japan
[3]Department of Biology, Faculty of Education and Integrated Arts and Sciences, Waseda University, Tokyo, Japan
[4]Integrative Bioscience and Biomedical Engineering, Graduate School of Advanced Science and Engineering, Waseda University, Tokyo, Japan
[5]Center for Regenerative Medicine, National Research Institute for Child Health and Development, Tokyo, Japan
[6]Department of Maternal-Fetal Biology, National Research Institute for Child Health and Development, Tokyo, Japan
[7]Department of Laboratory Medicine, St. Marianna University School of Medicine, Kawasaki, Kanagawa, Japan
[8]Department of Chemistry and Biological Science, Aoyama Gakuin University, Sagamihara, Kanagawa, Japan
[9]Laboratory of Bioresources, National Institute for Basic Biology, Okazaki, Aichi, Japan
[10]Children Cancer's Center, Division of Hematology, National Center for Child Health and Development, Tokyo, Japan
[11]Division of Endocrinology and Metabolism, National Center for Child Health and Development, Tokyo, Japan
[12]Department of Genome Medicine, National Research Institute for Child Health and Development, Tokyo, Japan
[13]Department of Molecular and Developmental Biology, Institute of Medicine, University of Tsukuba, Tsukuba, Ibaraki, Japan
[14]Division of Immunology, National Center for Child Health and Development, Tokyo, Japan
[15]Center for Postgraduate Education and Training, National Center for Child Health and Development, Tokyo, Japan

Twitter Kosuke Taniguchi @KosukeTaniguch2

Acknowledgements We would like to express our sincere gratitude to the staff of the National Center for Child Health and Development for their aid in treating the patients. We are grateful to NBRP Medaka (https://shigen.nig.ac.jp/medaka/) for providing OK-Cab (Strain ID: MT830) and Hatching Enzyme.

Contributors IT, SN and AIshiguro conceived the study and drafted the manuscript. KT-N, TS and HA participated in designing and coordinating the study, carried out molecular genetic studies and drafted the manuscript. AO, KN and TKato participated in the study design, carried out the animal experiments and drafted the manuscript. IT, AIguchi, HS, KA and AIshiguro collected the clinical data of the patients. MKashima, TY, HH, JT, HM and MKobayashi participated in the study design and coordination and carried out the animal experiments. OM, KT and KH participated in the genetic analysis and study design and helped draft the manuscript. TU and TKawai performed immunological studies. YN performed the endocrinological studies. TS, KM, KH and KA supervised the study and added important intellectual content. All authors critically revised the manuscript, commented on the drafts and approved the final draft.

Funding This study was supported by the Initiative on Rare and Undiagnosed Diseases grants (JP21ek0109489, 22bm0804017h0003) (KH and HA, respectively) from the Japanese Agency for Medical Research and Development; MEXT KAKENHI

(grant JP21K07787) (IT); and a national Grant-in-Aid from the National Center for Child Health and Development from the Japanese Ministry of Health, Labour, and Welfare (grants 2019 A-3, 2020B-3 and 2020B-10) (KA, SN and IT, respectively).

Competing interests None declared.

Patient consent for publication Consent obtained directly from patient(s).

Ethics approval This study involves human participants and was approved by the Ethics Committee of the National Center for Child Health and Development (#378). Participants gave informed consent to participate in the study before taking part.

Provenance and peer review Not commissioned; externally peer reviewed.

Data availability statement The datasets generated and/or analysed during the current study are available from the corresponding author on reasonable request.

ORCID iDs
Ayame Ogawa http://orcid.org/0009-0002-9282-8958
Kosuke Taniguchi http://orcid.org/0000-0003-1562-3764
Akira Ishiguro http://orcid.org/0000-0002-3896-5313

REFERENCES

1 Bellelli R, Borel V, Logan C, *et al*. Polε instability drives replication stress, abnormal development, and tumorigenesis. *Mol Cell* 2018;70:707–21.
2 Pachlopnik Schmid J, Lemoine R, Nehme N, *et al*. Polymerase E1 Mutation in a human syndrome with facial dysmorphism, immunodeficiency, Livedo, and short stature ("FILS syndrome. *J Exp Med* 2012;209:2323–30.
3 Thiffault I, Saunders C, Jenkins J, *et al*. A patient with polymerase E1 deficiency (Pole1): clinical features and overlap with DNA breakage/instability syndromes. *BMC Med Genet* 2015;16:31.
4 Logan CV, Murray JE, Parry DA, *et al*. DNA polymerase epsilon deficiency causes image syndrome with variable immunodeficiency. *Am J Hum Genet* 2018;103:1038–44.
5 Shima H, Koehler K, Nomura Y, *et al*. Two patients with Mirage syndrome lacking haematological features: role of somatic second-site reversion Samd9 mutations. *J Med Genet* 2018;55:81–5.
6 Kennedy RD, D'Andrea AD. The Fanconi anemia/BRCA pathway: new faces in the crowd. *Genes Dev* 2005;19:2925–40.
7 Ceccaldi R, Parmar K, Mouly E, *et al*. Bone marrow failure in Fanconi anemia is triggered by an exacerbated P53/P21 DNA damage response that impairs hematopoietic stem and progenitor cells. *Cell Stem Cell* 2012;11:36–49.
8 Dutt S, Narla A, Lin K, *et al*. Haploinsufficiency for Ribosomal protein genes causes selective activation of P53 in human erythroid progenitor cells. *Blood* 2011;117:2567–76.
9 Barlow JL, Drynan LF, Hewett DR, *et al*. A P53-dependent mechanism underlies macrocytic anemia in a mouse model of human 5Q- syndrome. *Nat Med* 2010;16:59–66.
10 Le Goff S, Boussaid I, Floquet C, *et al*. P53 activation during Ribosome Biogenesis regulates normal erythroid differentiation. *Blood* 2021;137:89–102.

Supplemental Data

Detailed clinical descriptions of the patients

Patient 1

Congenital anaemia

A Japanese female patient followed up for intrauterine growth restriction (IUGR) was born at 29 weeks of gestation with a weight of 726 g (−3.3 standard deviation [SD]) and a height of 32 cm (−2.9 SD). Her Apgar score at 5 min was 6. She did not require surfactant replacement therapy, but was on a ventilator for 9 days. Her haematological characteristics are shown in Supplemental Table 1 and Supplemental Figure 1. At birth, she had severe macrocytic anaemia without reticulocytopenia (red blood cells [RBC] 0.95 × 10^{12}/L, haemoglobin [Hgb] level 43 g/L, mean corpuscular volume [MCV] 123 fL, reticulocyte counts 158 × 10^{9}/L, white blood cells [WBC] 2.3 × 10^{9}/L, and platelets 396 × 10^{9}/L). Although she was treated with oral iron supplementation and erythropoietin administration with intermittent transfusion of packed RBC considering anaemia of prematurity, her anaemia did not improve. Oral iron supplementation and erythropoietin administration were discontinued in early infancy. She required repetitive transfusions of RBC once or twice a month. WBC counts (including differential counts) and platelets were normal (Supplemental Figure 1). Reticulocyte counts were mostly within the reference interval, but without marked reticulocytopenia in contrast to those observed in Diamond-Blackfan anaemia (DBA). She was referred to the National Center for Child Health and Development (Tokyo, Japan) during infancy for the evaluation and treatment of anaemia and bloody diarrhoea (details of gastrointestinal symptoms are described below). The examination of bone marrow aspirate revealed erythroid dysplasia, but without marked erythroid hypoplasia (M/E ratio 1.5) (Supplemental Table 1). These findings did not fit the diagnosis of DBA. Immunostaining for TP53 of bone marrow cells showed enhanced signals (Figure 1). The panel sequencing for known DBA-associated genes, including *RPS10, RPS14, RPS17, RPS19, RPS24, RPS26, RPL5, RPL11, RPL35A,* and *TP53*, did not detect any pathogenic variant. In toddlerhood, the follow-up bone marrow test demonstrated hypercellularity and revealed dysplasia of trilineage cells with excess blasts (7.5%) that fit myelodysplastic syndrome (MDS), classified into refractory anaemia with excess blasts

(RAEB)-1 using the World Health Organization (WHO) classification. G-banding karyotyping of the bone marrow aspirate showed a normal female karyotype as 46,XX.

Inflammatory bowel disease

The patient developed chronic bloody diarrhoea and underwent lower gastrointestinal endoscopy during infancy. Inflammatory bowel disease (IBD) (unclassified) was diagnosed based on the endoscopic and pathological findings. Her IBD was intractable to 5-aminosalicylate and exclusive enteral nutrition. Although it responded to corticosteroids, bloody diarrhoea relapsed soon after the discontinuation of corticosteroids. She was dependent on corticosteroids and required a central intravenous catheter for intravenous hyperalimentation to treat malnutrition caused by IBD.

Other clinical features

She had facial dysmorphism with epicanthic folds. She had no nail dystrophy, skin pigmentation, genitourinary anomalies, or café-au-lait patches. Despite adequate caloric intake, she showed no catch-up growth, and her height SD score was –3.1 SD (height 74 cm) in toddlerhood. At this point, hormone-secreting capacities of the anterior pituitary gland and adrenal cortex were investigated, but no abnormalities were found. Magnetic resonance imaging (MRI) showed microencephaly and skull thickening, and a computed tomography (CT) scan detected calcification at the right brachiocephalic artery. Her development was mildly delayed; she began to roll, sat steady, and crawled in late infancy, and walked in late toddlerhood. In early childhood, she could run, use several words, and imitate actions, but could not use two-word phrases, build a tower of two bricks, use a spoon, or express wants with pointing. Clinical features compared to those of FILS and IMAGE-I syndromes are shown in Supplemental Table 2.

Patient 2

Congenital anaemia

Patient 2, the younger female sibling of Patient 1, was born at 37 weeks of gestation with a weight of 2,124 g (–1.6 SD) and height of 43 cm (–1.9 SD). She had a low Apgar score (4 at 5 min) and required

ventilator support for 2 days. She also had epicanthic folds resembling her sibling's. Her haematological characteristics are shown in Supplemental Table 1 and Supplemental Figure 2. Her Hgb level was 54 g/L at birth, there were no decreases in reticulocyte counts, WBC counts, or platelet counts (RBC 1.71×10^{12}/L, MCV 117 fL, reticulocyte counts 30×10^{9}/L, platelets 306×10^{9}/L, and WBC 12.8×10^{9}/L). Bone marrow examination in infancy showed erythroid dysplasia, but without marked erythroid hypoplasia (M/E ratio 1.5) (Supplemental Table 1). Immunostaining for TP53 of bone marrow cells showed enhanced signals (Figure 1). She required repetitive transfusions of packed RBC once or twice a month. In early toddlerhood, the follow-up examination of the bone marrow aspirate demonstrated hypercellularity and dysplasia of trilineage cells with excess blasts (8.0%) that fit MDS, classified into RAEB-1. G-banding karyotyping showed a normal female karyotype as 46,XX.

Other clinical features

She had no nail dystrophy, skin pigmentation, genitourinary anomalies, or café-au-lait patches. She showed growth failure with height 71 cm (–2.6 SD) in toddlerhood. At this point, hormone-secreting capacities of the anterior pituitary gland and adrenal cortex were investigated, but no abnormalities were found. She showed the following typical developmental milestone achievements: began to roll, sat alone, walked, and used words during infancy. In toddlerhood, considering the abnormal intracranial findings of Patient 1, brain MRI, MR angiography, and CT scans of head, chest, and abdomen and pelvis were performed, showing no abnormal findings. Clinical features compared to those of FILS and IMAGE-I syndromes are shown in Supplemental Table 2.

She had not developed bloody diarrhoea by the follow-up period. She underwent a colonoscopy for her mild diarrhoea during infancy, but endoscopic and pathological findings of IBD were not detected.

Supplemental methods:

Immunostaining of bone marrow samples

Clot sections of the bone marrow obtained from Patient 1, Patient 2, and controls (a patient with

immune thrombocytopenia in early childhood and a patient with autoimmune neutropenia in infancy) were treated with high pH target retrieval solution (Dako, Santa Clara, CA) at 98 °C for 40 min. Immunostaining was performed with mouse anti-TP53 antibody (DO-7, Dako Nichirei Bioscience, Tokyo, Japan) and a polymer reagent Simple Stain MAX-PO (MULTI; Nichirei Bioscience) in an autostainer, i.e., Histostainer (48A, Nichirei Bioscience), for 30 min at room temperature.

Exome sequencing

Genomic screening was conducted under the "Initiative for Rare and Undiagnosed Diseases in Paediatrics" program supported by the Japan Agency for Medical Research and Development after obtaining written informed consent from the patients' parents. Exome sequencing of the patients and their parents were performed with SureSelect Human All ExomeV6 (Agilent Technologies, Santa Clara, CA) and the Illumina HiSeq 2500 system (Illumina, San Diego, CA), as previously described.[1] We filtered the dataset using the Japanese variant database JPN38K (https://jmorp.megabank.tohoku.ac.jp). To obtain a list of candidate pathogenic variants, the following filtering criteria were applied: (1) non-synonymous or frameshift variants in coding exons or splicing sites, (2) allele frequencies below 0.5% in 38KJPN, and (3) absence of the variant in our in-house exome data to filter pipeline-specific systematic errors. Potential pathogenicity was assumed from inheritance patterns — *de novo*, homozygous, compound heterozygous, or hemizygous — and functional effects were predicted using SIFT, PolyPhen2, and CADD.

Direct sequencing was performed to confirm the presence of the identified *POLE* variants. The genomic DNA samples from the patients were PCR-amplified for the region containing the variant using AmpliTaq Gold 360 PCR Master Mix (Thermo Fisher Scientific, Waltham, MA). The PCR products were sequenced with BigDye Terminator v3.1 Cycle Sequencing Kit (Thermo Fisher Scientific) on an ABI 3130 sequencer (Thermo Fisher Scientific).

Functional characterization of POLE variants

A vector containing human *POLE* cDNA (FHC24944) was purchased from Kazusa DNA Research Institute (Chiba, Japan). We modified the pBQM812A-1 vector (System Biosciences, Palo Alto, CA)

by replacing the cumate-inducible promoter with a doxycycline-inducible promoter and the CymR repressor sequence with the reverse tetracycline transactivator sequence.[2] *POLE* cDNA was cloned into the modified vector by adding the haemagglutinin (HA) sequence to the N-terminus using the Gibson assembly technique (NEBuilder HiFi DNA Assembly Master Mix; New England Biolabs, Ipswich, MA). We introduced c.3392del and c.5672_5674del into the wildtype (WT)-POLE1-expressing vector using a standard PCR-based method. HEK293 cells were maintained in Dulbecco's modified Eagle's medium supplemented with 50 U/mL penicillin, 50 μg/mL streptomycin, and 10% foetal bovine serum (FBS). The cells were transfected with each vector using Lipofectamine 3000 reagent (Thermo Fisher Scientific), and inducible stable cell lines were established according to the protocol for pBQM812A-1.

For Western blotting, nuclear and cytoplasmic extracts were prepared from inducible stable HEK293 cells expressing each HA-POLE1 (WT, Asp1131fs or Thr1891del). The cells cultured in 10-cm dishes were treated with 1 μg/mL doxycycline for 24 h. The cells were harvested using 0.25% trypsin-ethylene diamine tetra acetic acid (EDTA) solution and centrifuged at 2,000 rpm for 3 min. Cell pellets were lysed in five times the pellet volume (PV) of hypotonic lysis buffer (10 mM Tris, pH 8.0, 1.5 mM $MgCl_2$, 10 mM KCl, and 1 mM dithiothreitol with a protease inhibitor cocktail) and allowed to swell on ice for 15 min. Triton X-100 was added to a final concentration of 0.6%, and the samples were vortexed for 10 seconds. The homogenates were pelleted by centrifugation at 10,000 × *g* for 30 seconds, and the supernatants were stored as cytoplasmic lysates. The nuclear pellets were suspended in extraction buffer (20 mM Tris pH 8.0, 1.5 mM $MgCl_2$, 420 mM NaCl, 0.2 mM EDTA, 25% glycerol, and 1 mM dithiothreitol with a protease inhibitor cocktail) at two-thirds volume of the PV and rotated for 15 min at 4 °C. The homogenates were centrifuged at 20,000 × *g* for 5 min, and the supernatants were stored as cytoplasmic lysates. Nuclear and cytoplasmic extracts were separated using 10% sodium dodecyl sulphate-polyacrylamide gel electrophoresis (SDS-PAGE). Immunoblotting was performed with rat anti-HA antibody (clone 3F10; Sigma-Aldrich, St. Louis, MO), rat anti-tubulin antibody (YL1/2; Abcam, Cambridge, UK) and rabbit anti-histone H3 antibody (ab1791; Abcam) as primary antibodies, and horseradish peroxidase (HRP)-conjugated goat anti-rat IgG (Sigma-Aldrich) and HRP-conjugated goat anti-rabbit IgG (Sigma-Aldrich) as secondary

antibodies.

To visualize subcellular localization of each HA-POLE1 protein (WT, Asp1131fs or Thr1891del), inducible stable HEK293 cells were seeded on glass-bottom dishes and grown with 1 μg/mL doxycycline for 24 h. The cells were then fixed in 4% formaldehyde in phosphate-buffered saline (PBS) at room temperature for 10 min. Blocking and plasma membrane permeabilization were performed by incubating the cells with 4% Block Ace (KAC, Kyoto, Japan) and 0.1% Triton X-100 at room temperature for 1 h. Immunofluorescence was performed using rat anti-HA antibody (clone 3F10) and rabbit anti-POLE2 antibody (HPA02755; Thermo Fisher Scientific) as primary antibodies, and Alexa Fluor 488-conjugated donkey anti-rat IgG antibody (A21208, Thermo Fisher Scientific) and Alexa Fluor 647-conjugated goat anti-rabbit IgG antibody (A27040; Thermo Fisher Scientific) as secondary antibodies. Nuclei were stained with Hoechst 33342 (Dojindo Laboratories, Kumamoto, Japan). The cells were observed under an FV3000 confocal microscope (Olympus, Tokyo, Japan).

Generation of patient-derived induced pluripotent stem cells (iPSCs)

Human iPSCs were generated and maintained on iMatrix-511 (Nippi, Inc., Tokyo, Japan) in StemFit AK02N (Reprocell, Inc., Kanagawa, Japan) or StemFlex (Thermo Fisher Scientific) media. For Patient 1, a small intestinal tissue biopsy specimen obtained from the patient was chopped into small pieces and seeded on a dish in DMEM/F12 (Thermo Fisher Scientific) containing 20% FBS. The medium was changed every 2 days until confluence. Intestinal epithelial cells were maintained in DMEM/F12 containing 20% FBS until reprogramming. On the first day of reprogramming, we changed the culture medium to NutriStem Medium (Sartorius Stedim Biotech, Göttingen, Germany) and used the StemRNA-3rd Gen Reprogramming Kit (Reprocell, Inc.) to induce six reprogramming factors, including OCT4, SOX2, KLF4, c-MYC, NANOG, and LIN28, following the manufacturer's protocol. From days 2-4, we replaced the fresh NutriStem medium and transfected a reprogramming cocktail using Lipofectamine RNAiMAX (Thermo Fisher Scientific) every day. From day 5, the old medium was changed every 2 days until colony pickup.

For Patient 2, peripheral blood mononuclear cells (PBMCs) were isolated from the whole blood of the patient by centrifugation on Ficoll-Paque gradient using Leucosep (Greiner Bio-One

International GmbH, Frickenhausen, Germany) following the manufacturer's protocol. The CytoTune-iPS 2.0 Sendai Reprogramming Kit (Thermo Fisher Scientific) was used to induce four reprogramming factors, including OCT4, SOX2, KLF4, and L-MYC. PBMCs were infected with Sendai virus vector at 37 °C in a 5% CO_2 incubator for 2 h. Next, the infected PBMCs were seeded into iMatrix-511-coated 12-well plates (AGC Techno Glass Co., Ltd., Shizuoka, Japan) in KBM 501 medium (Kohjin Bio Co., Ltd., Saitama, Japan) with 10% FBS (Thermo Fisher Scientific). On days 2 and 4, 1 mL of StemFit AK02N medium was added gently to avoid disturbing cell adhesion, after which the entire medium was changed every 2 days until colony pickup.

From days 14-21, individual colonies were picked into iMatrix-511-coated 4-well plates (Thermo Fisher Scientific) in StemFit AK02N medium supplemented with 10 μM Y-27632 (Fujifilm Wako Pure Chemical Corporation, Osaka, Japan) or in StemFlex medium supplemented with 10 μM Y-27632. The medium was changed every other day and cells were passaged approximately once per week using enzymatic (TrypLE Select Enzyme or Accutase Cell Dissociation Reagent; Thermo Fisher Scientific) or mechanical methods.

RNA sequencing (RNA-seq) analysis

Total RNA was extracted from the iPSCs generated from the *POLE* variant carriers and control individuals (three lines for Patient 1, one line for Patient 2, and one line each from the two controls) using TRIzol reagent (Thermo Fisher Scientific) following the manufacturer's instructions. The RNA samples were treated with TruSeq Stranded Total RNA Library Prep Kit (Illumina), and the libraries were sequenced on DNBSEQ-T7 (MGI Tech Co., Ltd., Shenzhen, China). Reads were aligned to the reference human genome hg38, visualized with Integrative Genomics Viewer (https://software.broadinstitute.org/software/igv/), and reads per gene were counted using STAR-2.7.9a software.[3] Within-sample normalization was conducted using the fragments per kilobase million method, and between-sample normalization was performed using the trimmed mean of the M-values method.[4]

Western blotting of TP53 protein

For Western blotting, nuclear proteins were extracted from iPSCs generated from the patients, and normal controls (two iPSC lines each). First, the cells grown in 10-cm dishes were harvested using 0.25% trypsin-EDTA solution and centrifuged at 2,000 rpm for 3 min. Cell pellets were lysed in five times the PV of hypotonic lysis buffer (10 mM Tris, pH 8.0, 1.5 mM $MgCl_2$, 10 mM KCl, and 1 mM dithiothreitol with a protease inhibitor cocktail) and allowed to swell on ice for 15 min. Triton X-100 was added to a final concentration of 0.6%, and the samples were vortexed for 10 s. The homogenates were pelleted by centrifugation at 10,000 × *g* for 30 seconds and the supernatants were discarded. The nuclear pellets were suspended in extraction buffer (20 mM Tris pH 8.0, 1.5 mM $MgCl_2$, 420 mM NaCl, 0.2 mM EDTA, 25% glycerol, and 1 mM dithiothreitol with a protease inhibitor cocktail) at two-thirds volume of the PV and rotated for 15 min at 4 °C. The homogenates were centrifuged at 20,000 × *g* for 5 min, and the supernatants (nuclear fraction) were separated using 10% SDS-PAGE. Immunoblotting was performed with mouse anti-TP53 antibody (DO-7) and rabbit anti-histone H3 antibody (ab1791) as primary antibodies, and HRP-conjugated goat anti-mouse IgG (Sigma-Aldrich) and HRP-conjugated goat anti-rabbit IgG (Sigma-Aldrich) as secondary antibodies.

Generation of Pole-deficient medaka

Supplemental Figure 3 shows the sequence alignment of human and medaka *Pole* orthologues. We designed two crRNAs that recognize the sequences ACG TAG AAT ACA TCA CCA AC (site 1) and GAA TAC ATC ACC AAC AGG TC (site 2) of the medaka DNA polymerase epsilon (*Pole*) gene to establish a *Pole* mutant using CRISPR/Cas9. Partial sequences of medaka *Pole*, two crRNA recognition sites, and PCR primers for the amplification of the target region are shown in Supplemental Figure 4. The formation of duplex guide ribonucleoproteins (dgRNP) is in accordance with that reported by Hoshijima *et al*.[5] The crRNA, tracrRNA, and Cas9 proteins were purchased from Integrated DNA Technologies (IA). The PCR primers (CAT CTT GTG CAC CAA AAA GC and AAG TCT TGG GGT TTT GAA AT) were purchased from Fasmac (Kanagawa, Japan). Microinjection and establishment of *Pole* knockout strains are in accordance with "Medaka: Biology, Management, and Experimental Protocol, Volume 2".[6] Briefly, microinjected with dgRNPs into embryos at the 1 cell stage, eggs were incubated for 4 days at 25 °C, and the genomic DNA was extracted and subjected to

PCR amplification. The efficiency of genome editing was evaluated using an automated electrophoresis system MCE-202 with a DNA-500 reagent kit (Shimadzu, Kyoto, Japan). Two dgRNPs were designed to efficiently edit the target DNA regions. Following the selection of four pairs of founder fish, we observed the phenotypes of the next generation. Two out of the four pairs of founder fish laid eggs with a specific phenotype. We selected four founder fish, No. 5, No. 6, No. 7, and No. 8, and mated them with WT fish. Supplemental Figure 5 shows the types of insertions or deletions identified in the target region of the F1 fish using amplicon sequencing. As a result, we established two mutant lines, one with a 4 bp deletion mutation using one crRNA (site 2) and another with a 9 bp deletion mutation using another crRNA (site 1) at the *Pole* gene. We named these two mutant strains *Pole^del4* and *Pole^del9*, respectively. Two mutant strains *Pole^del4* and *Pole^del9* showed essentially similar phenotypes, and thus we used the *Pole^del9* strain for further analysis. As shown in Supplemental Figure 4, the *Pole^del9* strain deleted the splice-acceptor site and was expected to be non-functional.

Morphological observation of medaka

Medaka has a more extended period time from fertilization to hatching than zebrafish. For this reason, the length of the body and other developmental phenotypes in pre-hatched embryos cannot be accurately analysed. Therefore, we dissolved the chorion using hatching enzymes[7,8] and observed the embryos. The hatching enzyme was supplied by NBRP Medaka (https://shigen.nig.ac.jp/medaka/). Seven days after fertilization, the eggs were transferred to waterproof sandpaper (#1200) (AS One, Osaka, Japan) placed in the lid of a 10-cm Petri dish. Breeding water was removed, and a moderate amount of Iwamatsu's balanced salt solution (BSS)[9] was added to prevent the drying of the eggs. The eggs were slowly rolled to remove outer surface hairs and lightly scratch the surface of the eggs. The eggs were then transferred to a 24-well plate, and the BSS was removed. The hatching enzyme diluted three times in BSS was added so that the eggs were immersed and incubated at 27 °C. As soon as the embryos emerged from the chorion, embryos were transferred to a Petri dish containing 1 × BSS. The embryos were captured using a microscope camera (Zeiss Axiocam 208 colors; Carl Zeiss Meditec, Jena, Germany) attached to a stereomicroscope (model M165C; Leica, Wetzlar, Germany).

Blood cell counts of medaka

Following anaesthesia with tricaine methane sulfonate (MS222; Sigma-Aldrich), the fish's heart was exposed by dissection. Blood was collected from the bulbus arteriosus using glass capillaries (GD-1; Narishige, Tokyo, Japan) coated with 10,000 U/mL heparin sodium salt (Wako, Osaka, Japan).[10] In our experiments, we used Dulbecco's modified PBS (DPBS), treated to remove Mg^{2+} and Ca^{2+} ions [DPBS (–)] to prevent coagulation during the dilution of whole blood when necessary. Total blood cells were diluted to 1:200, stained with Shaw's diluent, and counted using a haemocytometer.[11] Blood cells (2×10^5 cells) diluted in DPBS (–) containing 2.5% FBS were centrifuged (Cytopro 7620; Wescor Inc., Logan, UT) at 1,000 rpm for 4 min to prepare cell centrifuge specimens and transferred onto glass slides. After air drying, cells were stained with o-dianisidine (Wako) and Giemsa (Wako) as previously described.[12] Blood cells were examined by light microscopy (model BX51; Olympus, Tokyo, Japan).

Statistical analysis

Data were analysed using the GraphPad Prism 9.1.2 software (GraphPad Software, Inc., San Diego, CA). The two-group datasets were analysed using Student's *t*-test. Statistical significance was set at $P < 0.05$.

References

1. Sato T, Samura O, Kato N, et al. Novel TFAP2A mutation in a Japanese family with branchio-oculo-facial syndrome. *Hum Genome Var* 2018;5:5.

2. Shima H, Koehler K, Nomura Y, et al. Two patients with MIRAGE syndrome lacking haematological features: role of somatic second-site reversion SAMD9 mutations. *J Med Genet* 2018;55:81–5.

3. Dobin A, Davis CA, Schlesinger F, et al. STAR: ultrafast universal RNA-seq aligner. *Bioinformatics* 2013;29:15–21.

4. Robinson MD, Oshlack A. A scaling normalization method for differential expression analysis of RNA-seq data. *Genome Biol* 2010;11:R25.

5. Hoshijima K, Jurynec MJ, Klatt Shaw D, et al. Highly efficient CRISPR-Cas9-based methods for generating deletion mutations and F0 embryos that lack gene function in Zebrafish. *Dev Cell* 2019;51:64–557.e644.

6. Murata K, Kinoshita M, Naruse K, et al. Heteroduplex mobility assay – A simple method to detect targeted genome modification. In: Murata K, Kinoshita M, Naruse K, et al. eds. Medaka: Biology, Management, and Experimental Protocols. Vol. 2. Iowa: Wiley-Blackwell 2019:244–60.

7. Kinoshita M, Murata K, Naruse K, et al. Medaka: biology, management, and experimental protocols. New York: John Wiley & Sons 2009:252–56.

8. Porazinski SR, Wang H, Furutani-Seiki M. Dechorionation of medaka embryos and cell transplantation for the generation of chimeras. *J Vis Exp* 2010;46:e2055.

9. Iwamatsu T. A new technique for dechorionation and observations on the development of the naked egg in Oryzias latipes. *J Exp Zool* 1983;228:83–9.

10. Kayo D, Oka Y, Kanda S. Examination of methods for manipulating serum 17β-estradiol (E2) levels by analysis of blood E2 concentration in medaka (Oryzias latipes). *Gen Comp Endocrinol* 2020;285:113272.

11. Hadji-Azimi I, Coosemans V, Canicatti C. Atlas of adult Xenopus laevis laevis hematology. *Dev Comp Immunol* 1987;11:807–74.

12. Okui T, Yamamoto Y, Maekawa S, et al. Quantification and localization of erythropoietin-receptor-expressing cells in the liver of Xenopus laevis. *Cell Tissue Res* 2013;353:153–64.

Supplemental Tables

Supplemental Table 1. Haematological characteristics of the two patients in our study

	Patient 1				Patient 2			
	At birth	Infancy	Early toddler	Toddler	At birth	Infancy	Early toddler	Toddler
Height, cm, SD	32, −2.9	52, −6.0	67, −4.0	74, −3.1	43, −1.9	54, −2.5	66, −3.3	71, −2.6
Weight, g	726	3550	8210	11,750	2124	4465	7315	7945
BMI, SD	7, −5.2	13, −3.1	18, 1.9	21, 4.0	11, −1.0	15, −0.9	17, 0.5	16, 0.1
Laboratory findings								
Hgb, g/L	43	77*	64*	84*	54	70*	79*	67*
RBC, 10^{12}/L	0.95	2.48*	1.89*	2.70*	1.71	2.49*	2.09*	2.05*
MCV, fL	123.0	97.5	102.8	95.3	116.8	84.7	115.5	101.7
MCH, pg	45.1	31.2	33.8	31.1	32.4	27.9	37.6	32.4
MCHC, g/L	365	320	328	326	278	330	326	319
Reticulocytes, %, 10^9/L	16.6, 158	2.1, 51	2.9, 55	2.0, 53	1.7, 30	1.4, 27	0.4, 9	9.9, 203
Platelets, 10^9/L	396	929	465	418	306	670	474	283
WBC, 10^9/L	2.3	14.7	4.1	5.9	12.8	4.81	7.16	4.67
Neutrophils, 10^9/L	0.7	9.6	2.2	5.2	6.6	2.0	2.9	2.4
Lymphocytes, 10^9/L	1.3	4.6	1.7	0.5	3.6	2.2	3.4	2.0
Eosinophils, 10^9/L	0.0	0.1	0.1	0.0	0.2	0.3	0.4	0.3
Monocytes, 10^9/L	0.3	0.4	0.1	0.2	1.2	0.3	0.4	0.2
LDH (U/L)	565	293	263	352	2205	331	449	340
Total bilirubin (mg/L)	28.0	2.7	3.5	3.6	26.0	5.9	9.7	7.9
Bone marrow findings								
Cellularity		Normo-	Hyper-	Hyper-		Normo-	Hyper-	Hyper-
M:E ratio		1.5	0.5	2.0		1.5	0.9	1.5
Blasts, %		3.6	1.0	7.5		1.6	8.0	4.2
Dysplastic changes								
Erythroid cells		+	+	+		+	+	+
Myeloid cells		–	+	+		–	+	+
Megakaryocytes		–	+	+		–	+	+
G-banding	46,XX				46,XX			
Chromosome breakage testing	NA				Negative			

BMI, body mass index; Hgb, haemoglobin; LDH, lactate dehydrogenase; MCH, mean corpuscular haemoglobin; MCHC, mean corpuscular haemoglobin concentration; MCV, mean corpuscular volume; M:E, myeloid:erythroid; NA, not available; RBC, red blood cells; SD, standard deviation; WBC, white blood cells.

* Hgb levels and red blood cell counts were modified due to repetitive transfusion of red blood cells.

+ Dysplastic changes were detected. – Dysplastic changes were not detected.

Supplemental Table 2. Immunological characteristics of the two patients in our study

	Patient 1 (Infancy)	Reference interval	Patient 2 (Toddler)	Reference interval
Absolute lymphocyte count (cells/μL)	1200	(3400-9000)*	2400	(3600-8900)*
Lymphocyte subsets				
$CD3^+$ T cells (/μL, %)	690, 58	(1900-5900, 49-76)*	1169, 49	(2100-6200, 53-75)*
$CD4^+$ T cells (/μL, %)	576, 48	(1400-4300, 31-56)*	698, 29	(1300-3400, 32-51)*
$CD8^+$ T cells (/μL, %)	90, 7	(500-1700, 12-24)*	217, 9	(620-2000, 14-30)*
$CD19^+$ B cells (/μL, %)	341, 28	(610-2600, 14-37)*	240, 10	(720-2600, 16-35)*
$CD16^+$ $CD56^+$ NK cells (/μL, %)	110, 9	(160-950, 3-15)*	941, 39	(180-920, 3-15)*
Immunoglobulin profile				
IgG level (mg/dL)	377	(290-950)†	774	(470-1210)†
IgA level (mg/dL)	60	(8-50)†	39	(14-98)†
IgM level (mg/dL)	46	(46-176)†	65	(81-314)†

* Shearer WT, Rosenblatt HM, Gelman RS, et al. Lymphocyte subsets in healthy children from birth through 18 years of age: the Pediatric AIDS Clinical Trials Group P1009 study. J Allergy Clin Immunol.

† These reference ranges are derived from reference intervals of clinical tests in Japanese children (Tanaka T, Yamashita A, Ichihara K. 2008. Reference intervals of clinical tests in children determined by a latent reference value extraction method. J Jpn Pediatr Soc 112: 1117-1132 [in Japanese]).

CD, cluster of differentiation: NK, natural killer; Ig, immunoglobulin.

Supplemental Table 3. Clinical features of the two patients in our study compared to those with FILS and IMAGE-I syndromes

	Patient 1	Patient 2
FILS syndrome-compatible		
Facial dysmorphism	+	+
Immunodeficiency	–	–
Livedo	–	–
Short stature	+	+
IMAGE-I syndrome-compatible		
Intrauterine growth retardation	+	+
Metaphyseal dysplasia	+	–
Adrenal hypoplasia congenita	–	–
Genital anomalies	–	–
Immunodeficiency	–	–
Other features of our patients		
Congenital anaemia	+	+
Myelodysplastic syndrome	+	+
Inflammatory bowel disease	+	–
Microcephaly	+	–
Pulmonary fibrosis	–	–
Nail dystrophy	–	–
Teeth abnormality	–	–
Hypogammaglobulinemia	–	–
Splenomegaly	–	–

FILS, facial dysmorphism, immunodeficiency, livedo, and short stature; IMAGE-I, intrauterine growth restriction, metaphyseal dysplasia, adrenal hypoplasia congenita, genital anomalies and immunodeficiency

Suppl. Fig. 1

Patient 1

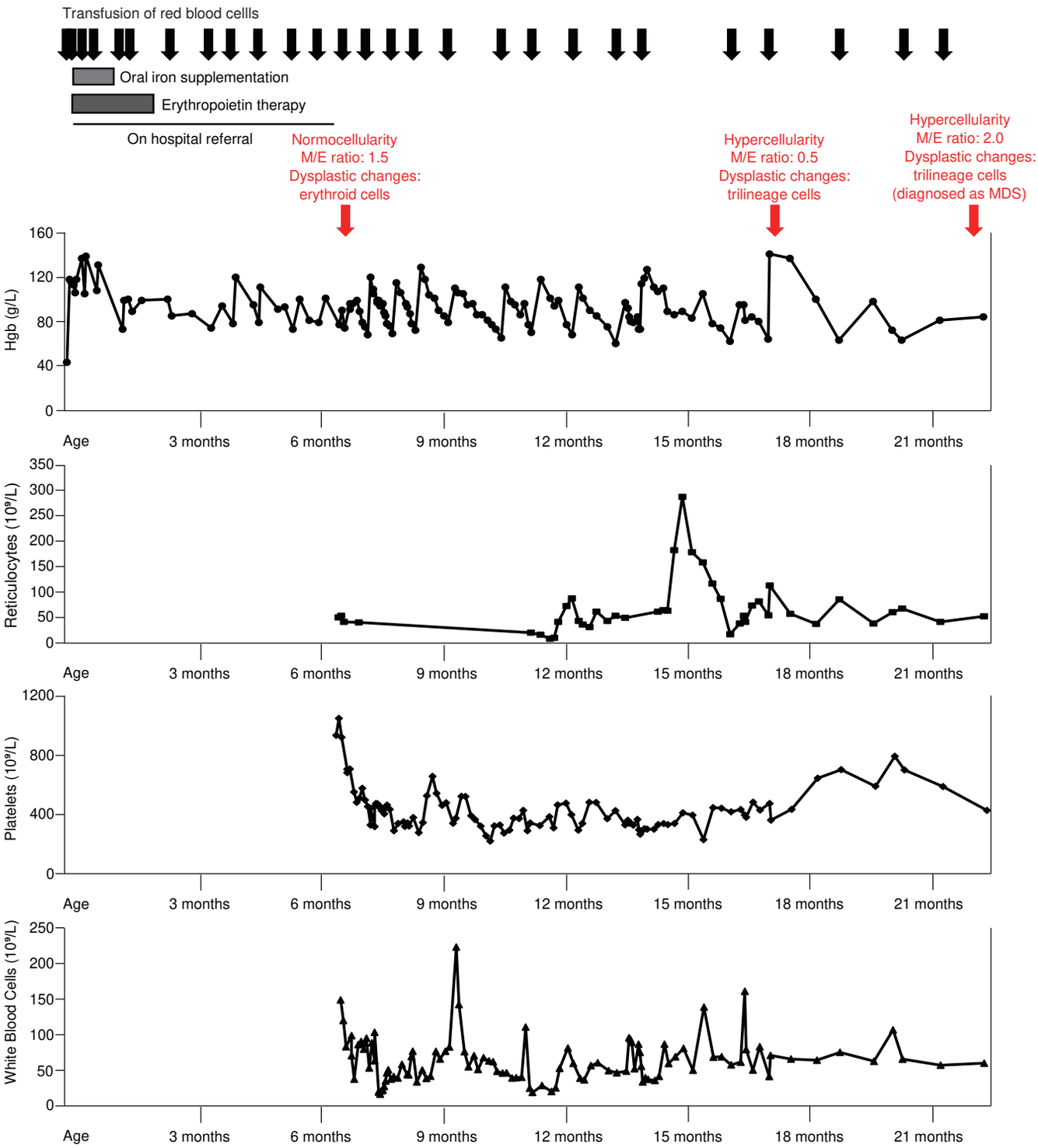

Suppl. Fig. 1: Changes in blood count in Patient 1 over time.

Suppl. Fig. 2

Patient 2

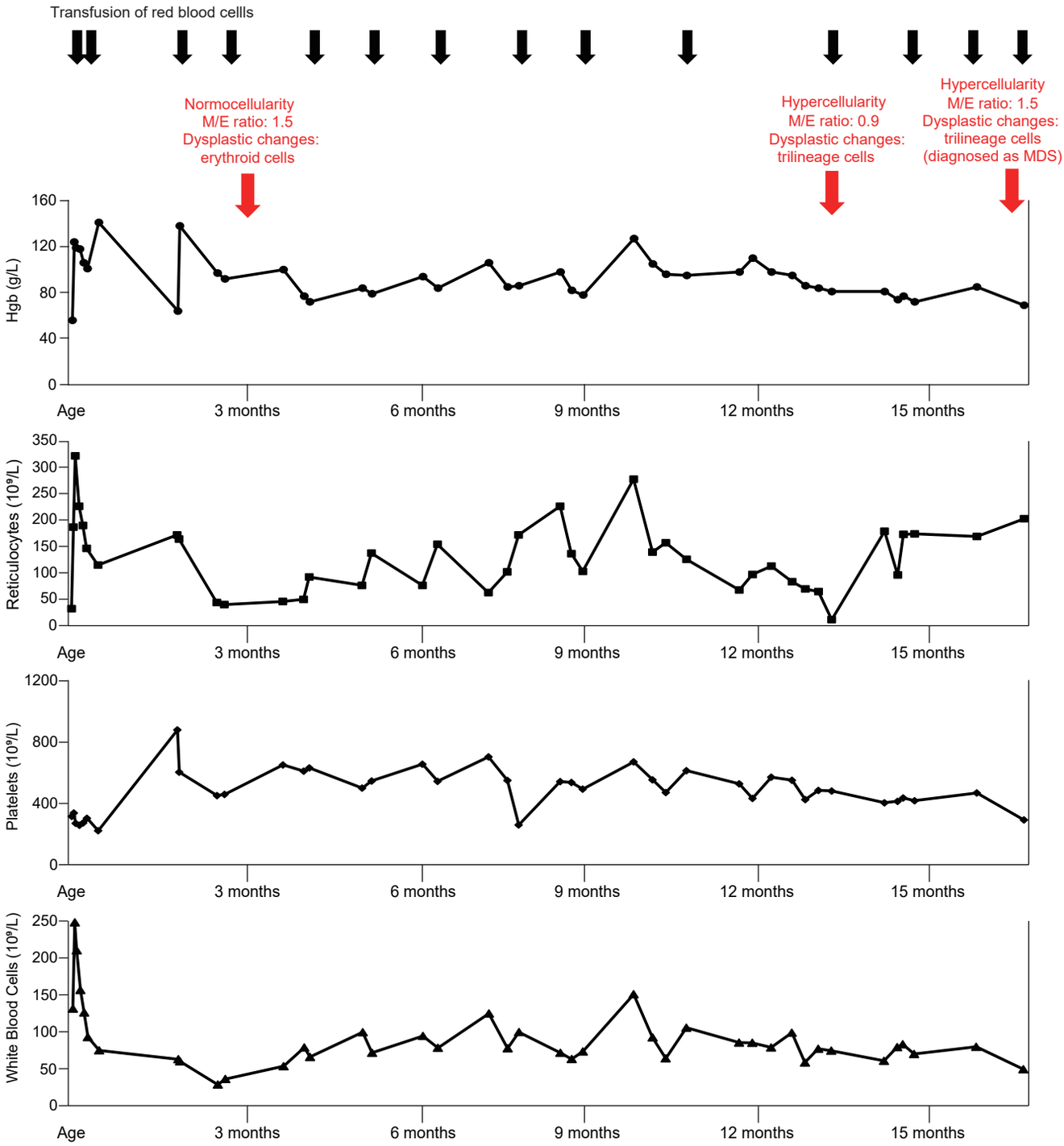

Suppl. Fig. 2: Changes in blood count in Patient 2 over time.

Suppl. Fig. 3

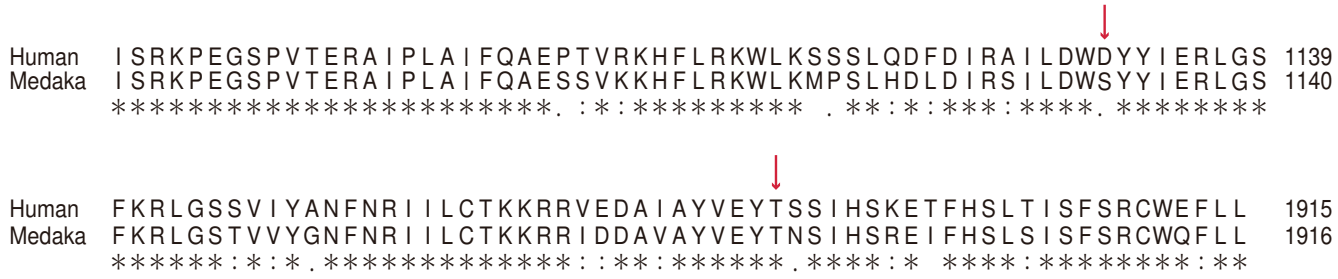

Suppl. Fig. 3: Sequence alignment of the human POLE1 and medaka orthologue. An asterisk (*) indicates identical amino acids, a dot (.) indicates a semi-conservative change, and a colon (:) represents a conservative change.

Suppl. Fig. 4

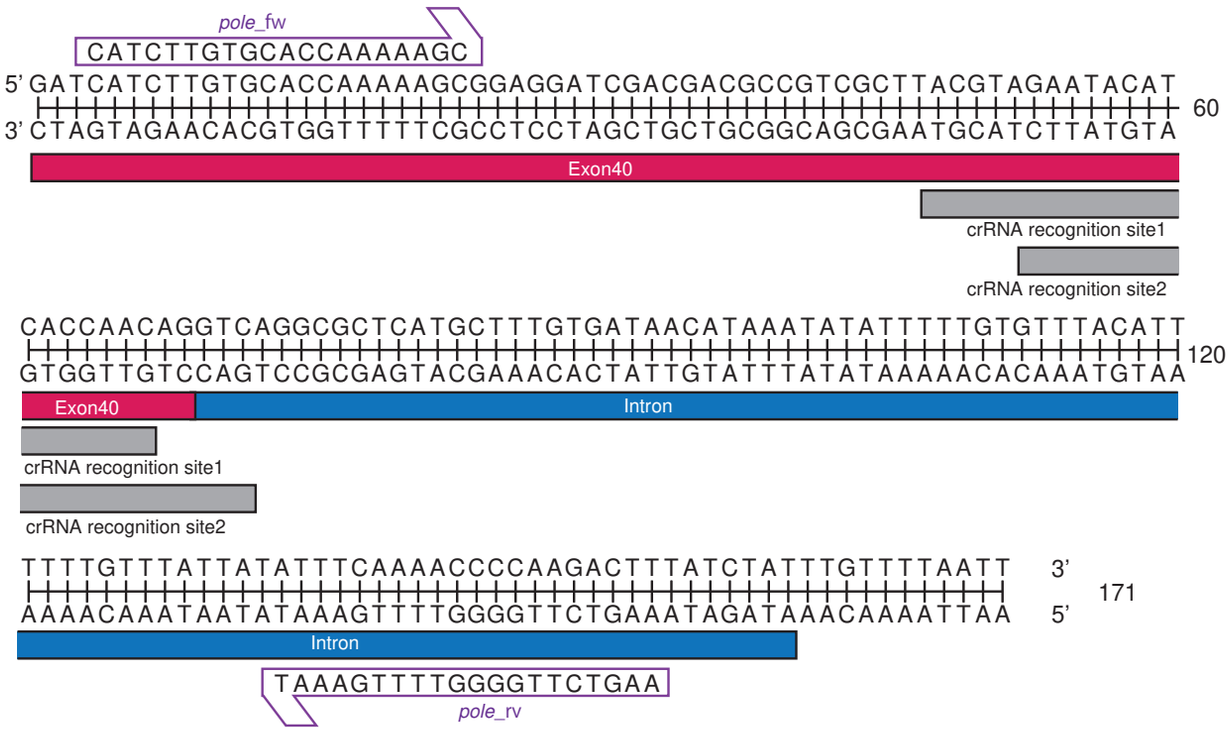

Suppl. Fig. 4: Partial sequence of pole, crRNA recognition sites 1 and 2, and primers for amplification of the target region.

Suppl. Fig. 5

			No. of F1 fish with mutation
WT	TCGCTTACGTAGAATACATCACCAACAGGTCAGGCGCTCATGCTT		
No.5 F1	TCGCTTACGTAGAATACATCACCAACAGG-----CGCTCATGCTT	Δ5	6/24
No.5 F1	TCGCTTACGTAGAATACATCACCA--------GGCGCTCATGCTT	Δ8	6/24
No.6 F1	TCGCTTACGTAGAATACATCACCAACAGG---CATGCTCATGCTT	Δ3	3/16
No.6 F1	TCGCTTACGTAGAATACATCACCA---------TCGCTCATGCTT	Δ9	6/16
No.6 F1	TCGCTTACGTAGAATACATCACCAACAGG-----CGCTCATGCTT	Δ5	3/16
No.7 F1	TCGCTTACGTAGAATACATCACCAACAGG-----CGCTCATGCTT	Δ5	11/26
No.7 F1	TCGCTTACGTAGAAT----------TACGTAGGGCGCTCATGCTT	Δ10	7/26
No.8 F1	TCGCTTACGTAGAATACATCAC----AGGTCAGGCGCTCATGCTT	Δ4	11/22

Suppl. Fig. 5: Type of deletions or insertions detected in F1 fish. Sequence analysis of the deletion and insertion induced by CRISPR/Cas9 genome editing. Two types of mutations from No.5, 3 types of No.6, 3 types of No.7 and 1 type of No.8 founder fish were detected. Two mutant lines were established; one has a 9 bp deletion from No.6 fish (named as pole1^E40del9) and another has a 4 bp deletion from No.8 fish (named as pole1^E40del4).